Safety and Reliability – Safe Societies in a Changing World – Haugen et al. (Eds)
© 2018 Taylor & Francis Group, London, ISBN 978-0-8153-8682-7

Effect of load-generation variability on power grid cascading failures

R. Rocchetta & E. Patelli
Institute for Risk and Uncertainty, Liverpool University, Liverpool, UK

L. Bing & G. Sansavini
Reliability and Risk Engineering Laboratory, Department of Mechanical and Process Engineering Institute of Energy Technology, ETH Zurich, Zurich, Switzerland

ABSTRACT: Cascading failures events are major concerns for future power grids and are generally not treatable analytically. For realistic analysis of the cascading sequence, dedicated models for the numerical simulation are often required. These are generally computationally costly and involve many parameters and variables. Due to uncertainty associated with the cascading failures and limited or unavailable historical data on large size cascading events, several factors turn out to be poorly estimated or subjectively defined. In order to improve confidence in the model, sensitivity analysis is applied to reveal which among the uncertain factors have the highest influence on a realistic DC overload cascading model. The 95*th* percentile of the demand not served, the estimated mean number of line failures and the frequency of line failure are the considered outputs. Those are obtained by evaluating random contingency and load scenarios for the network. The approach allows to reduce the dimensionality of the model input space and to identifying inputs interactions which are affecting the most statistical indicators of the demand not supplied.

1 INTRODUCTION

Assure high-reliability of electric power supply is a major concern for next-generation power grid. Power grid should have the ability to withstand know threats, such as N-1 and N-2 contingencies, but also poorly understood low-probability-high-consequence events such as N-k contingencies leading to cascading sequences. Due to the inherent complexity of cascading failure events, associated mathematical models are, generally, analytically not solvable. This is mainly due to the high dimensionality of the problem and to the complex, non-linear and dynamic behaviour characterizing domino failures.

Computational models for the simulation of the cascading sequences are used to provide a solution to the cascade problem. A wide variety of models have been proposed in the past, aiming at analysing different system behaviours and with several different objectives. For instance, models employing the AC power flow (PF) equations, such as the Manchester model (Nedic et al. 2006) or the linearized AC PF model (Li et al. 2016), the ORNL-PSerc-Alaska (OPA) model (Dobson, Carreras, Lynch, & Newman 2001) and DC PF-based models have been developed to simulate realistically cascading failures sequences.

Numerical models for cascading simulation have to be adequately designed, calibrated and validated (Bialek et al. 2016). Calibration and validation should use available historical cascading data, which is (in particular for large size cascade events) quite limited (Rocchetta et al. 2018) or affected by imprecision (Rocchetta et al. 2018). Consequently, the resulting model verification and calibration is very challenging and affected by high level of uncertainty. Uncertainty will result particularly prominent when the model is used to simulate rare events leading to very severe consequences.

To increase confidence in the cascading model results and better understand the relation between its inputs and outputs, all the relevant sources of uncertainty affecting the analysis should be quantified. Dimensionality and complexity issues are often involved in cascades analysis problems and the numerical simulators generally reflect these problems. In fact, the simulators often are time costly and involve a large number of uncertain variable and parameters.

Sensitivity analysis methods are useful to deal with both dimensionality and uncertainty issues. These methods can be used to reveal which sources of uncertainty are affecting the most the model output and can be used to reduce the dimensionality of the aleatory space by prioritizing only the most important factors. This is indeed a useful information, necessary to better comprehend inputs-outputs relations otherwise hidden within the complexity of the model.

Global sensitivity analysis methods are often employed by uncertainty analysts to sharpen the

view of the problem. Sensitivity analysis is sometimes regarded as a fundamental part of works that involves the assessment and propagation of uncertainty (Borgonovo and Plischke 2016). Applying global sensitivity analysis methods, insights can be gained regarding the input-output mapping and the key drivers of uncertainty can be clearly revealed (Borgonovo and Plischke 2016).

In this paper, an integrated framework for sensitivity analysis and power grids cascading analysis is proposed. The framework can be used to identify and prioritize the most relevant uncertain input factors by revealing their effect on different cascading failures indicators. Both system-level indicators, describing the overall impact of cascading failures, and component-level indicator, focusing on a single component performance, are considered. One of the aims of this work is to provide some guidance for the application of given data sensitivity analysis and screening methods to engineering practitioners, promoting their potential.

The framework is tested on a modified version of the RTS96 IEEE system. Two uncertainty cases are analysed, first accounting for only the uncertainty in the load demand. Then, a more complex and realistic case has been considered by accounting for randomness in the generators costs, thus inflating the dimensionality of the input space, i.e. more flexibility for the generators outputs. The analysis allows to point out which among loads and generator costs uncertainties is affecting the most the outputs of cascading failures model and for a modest computational effort.

The rest of the paper is organized as follows: Section 2 introduces global sensitivity analysis and screening methods. In Section 3 the algorithm for cascading failure simulation and the performance indicators are introduced. A benchmark case study, the RTS96 system, tests the framework in Section 4, 2 uncertainty cases are analysed. Section 5 closes the paper with a discussion on the results and conclusions.

2 SENSITIVITY ANALYSIS AND SCREENING

This section proposes a concise introduction to uncertainty quantification and methods for global sensitivity analysis. Traditionally, uncertainty quantification and analysis consist in the assignment of probability distributions to the model input factors (variables and parameters). Once the uncertainty has been characterized, it is propagated into the simulation code via Monte Carlo method. First, uncertain factors are characterised by assigning probability distributions. This is an important step which has to be performed adequately to assure high quality and consistency of results (Patelli, Pradlwarter, & Schuller 2010). Then, samples are obtained from the joint probability distribution of the input factors, e.g. by Latin hypercube sampling, quasi-random sequences or crude Monte Carlo inverse transform sampling (Patelli, Broggi, Angelis, & Beer 2014). Once the i^{th} input realisation is obtained $\boldsymbol{X}_i = \left[X_i(0),..,X_i(m)\right]$, the sample is forwarded to the computational model $M(X)$. This allows obtaining information about the input-output mapping defined by the computational model as follows:

$$M : \mathcal{X} \to \mathcal{Y},\ \boldsymbol{X} \to Y = M(\boldsymbol{X}) \tag{1}$$

where Y is the model output, for simplicity assumed 1-dimensional and without loss of generality.

Global sensitivity analysis methods have been developed to identify the most and the least relevant factors and gain additional insight on the input-output mapping defined in equation 1. Several global methods have been developed in the last decades. Screening methods, such as the one-at-a-time design of Morris (Morris 1991), variance-based methods, density-based methods (Borgonovo & Plischke 2016) are some of the most intensively applied methods.

2.1 *Given data Sobol's indices*

A variance-based statistic, commonly referred as the first order sensitivity coefficient, quantifies the (additive) effect of each input factor on the model output as follows (M. Sobol 1990):

$$S_i = \frac{V_{X_i}\left[\mathbb{E}_{\mathbf{X}_{-i}}[Y \mid X_i]\right]}{V[Y]} \tag{2}$$

where $V[Y]$ is the total variance of the output Y, X_i is the i^{th} uncertain input factor, $\mathbf{X}_{-i}$ is the matrix of all uncertain factors but X_i, $\mathbb{E}_{\mathbf{X}_{-i}}[Y \mid X_i]$, is the expectation of the model output Y taken over all possible values of $\mathbf{X}_{-i}$ while removing the X_i uncertainty (i.e. keeping X^i fixed) and $V_{X_i}[]$ is the variance taken over all possible values of X_i. The indices S_i can be used to reveal the importance of the input factor X_i on the variance of the output and it is a normalized index, that is $\sum_i S_i = 1$

The main effect index reveals what is the importance of each uncertain factor on the uncertainty in the model output. It relatively cheap to obtain as it can be efficiently computed using given data methods or from a single Monte Carlo run (Plischke et al. 2013). The main drawback of the index is that interactions between input factors are not accounted for with this sensitivity measure. Higher order Sobol's effects (second and higher order interactions) compose the so-called total effect index S_{Ti}. This is a variance-based measure of the influence of an input i accounting for all the inter-

actions with other uncertain factors. It is defined as follows:

$$S_{Ti} = \frac{\mathbb{E}_{\mathbf{X}_{\sim i}}\left[V_{X_i}[Y \mid \mathbf{X}_{\sim i}]\right]}{V[Y]} = 1 - \frac{V_{\mathbf{X}_{\sim i}}\left[\mathbb{E}_{X_i}[Y \mid \mathbf{X}_{\sim i}]\right]}{V[Y]} \tag{3}$$

where S_{Ti} account for all the contribution to the total variance of the output $V[Y]$ when the first order effect of $\mathbf{X}_{\sim i}$ is removed.

2.2 *Elementary effects and Morris diagram*

The Elementary Effects (EEs) is a screening method used identify the effect of input factors $X(i)$ with $i = 1,2,\ldots,m$ on the output Y of a mathematical or computational model $M(\mathbf{X})$. The method consists in the calculation of m incremental ratios, also called Elementary Effects, which are used to assess the influence of the input variables and parameters. The i^{th} elementary effect of the m-dimensional input vector $\mathbf{X}_0$ is defined as follows:

$$\delta_i(\mathbf{X}_0) = \frac{Y\left(X_0(1),.,X_0(i)+\Delta,.,X_0(m)\right) - Y(\mathbf{X}_0)}{\Delta} \tag{4}$$

where the quantity Δ is a given variation in the input factor whose effect has to be evaluated. Intuitively speaking, the input factors leading to the higher incremental ratios $\delta_i(\mathbf{X}_0)$ have to be considered as the most relevant for the output quantity Y. Of curse, this relevance metric is valid only locally, in $\mathbf{X}_0$, where Y has been evaluated. Repeated One-At-a-Time (OAT) evaluations of random vector configurations provide the elementary effect method with global sensitivity analysis features (Turati et al. 2017). The mean and standard deviation of the EEs, resulting from random input vector configurations, can be plotted in the well-known $\mu(\delta) - \sigma(\delta)$ plot proposed by Morris (Morris 1991). If a factor X_i results in a small absolute value of the mean and small variance, it should be considered less relevant for the model. On the other hand, a factor X_i resulting in a high $|\mu(\delta_i)|$ has to be considered highly relevant for the model, i.e. it leads to the average higher variation in the output. Similarly, a factor X_i resulting in a high $\sigma(\delta_i)$ is also of interest for the model output. In fact, high $\sigma(\delta_i)$ probably indicate a non-linear relation between the factor i and the output and/or a relevant interaction with other factors. An example of Morris plot is presented in Figure 1 where the standard error of the mean (SEM) is used to decompose the plot in different areas.

The method has some points of strength, worth highlighting: 1) It is relatively easy to implement; 2) Computationally cheap compared to other global sensitivity methods also for high number of factors; 3) It uses a sensitivity measure which is simple to communicate (similarity between incremental rations and partial derivatives) to non-experts; 4) Compared to variance/based measures, shows if the input factors are (in average) positively or negatively correlated to the output.

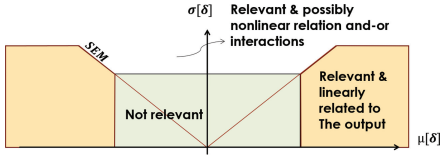

Figure 1. An example of Morris diagram and how to discern between important and non important factors.

3 THE CASCADING MODEL

A model for the simulation of steady-state operations of electric networks has been developed and calibrated in (Bing Li and Sansavini 2017). It can be used to simulate the initial contingencies that trigger the cascading events and estimate the post-contingency system states. The initial generation dispatch for each load demand is computed with a Security Constrained Optimal Power Flow (SCOPF), which takes into account the generators constraints, line flow constraints, voltage angles constraints and, optionally, the N-1 security constraints. After line tripping, DC power flow is used to evaluate the post-contingency power flow. The failures propagate in the grid through line over loading. Frequency control and protections, voltage protections and a variety of other automatic and realistic regulations and remedial actions are also included in the model.

A simplified flow chart of the cascading failures analysis is presented in Figure 2 adapted from (Bing Li and Sansavini 2017). The algorithm starts by loading power grid data, selecting the steady-state solver (e.g. DC-SCOPF) and a list of N-k contingencies. Then, for each contingency N-k, islands are identified, frequency deviation assessed and under frequency load shedding performed if necessary. Once power balance is restored, line flows are evaluated using the power flow solver and the lines exceeding their flow limit are removed from the grid topology. This process is repeated until grid stability is reached. The considered outputs are the total Demand-Not-Served (DNS) due to contingency N-k and lines failure indicator functions indicating if a line tripped during the simulation of the N-k contingency.

For simplicity, the contingency list has been obtained by random sampling N-1, N-2 and N-k line contingencies. To better identify and select

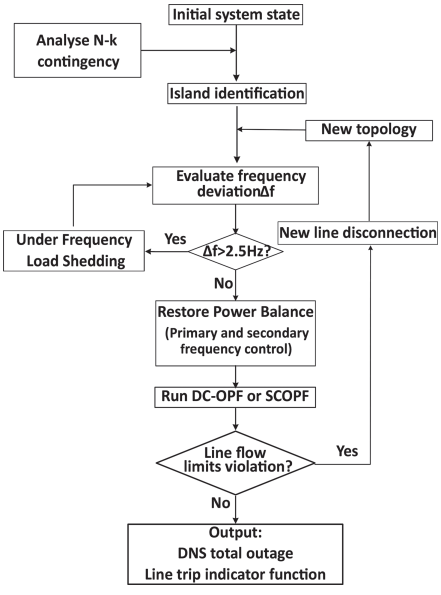

Figure 2. The flow chart of the algorithm for cascading failures analysis.

critical failure scenarios, methods such as the N-2 contingency screening, eg. the method presented in (Kaplunovich and Turitsyn 2016), could have been employed. However, a smart exploration of the contingency space was not the main aim of this work. Once the list is obtained, repeated N-k contingency analysis are performed as presented in Algorithm (Bing Li and Sansavini 2017).

3.1 *System and components performance indicators*

Several output measures can be obtained from the cascades model. In this work, we focus on 2 system-level indicators, which provide insights on the grid performance as a whole, and on N_l components performance indicators, one for each line in the system.

The indicators are the 95*th* percentile of the DNS cumulative distribution function $p_{95}(DNS)$, the average total number of lines tripped $\mu(N_f)$ and the line outage frequency $P_{f,l}$, defined as follows:

$$\mu(N_f) = \frac{\sum_{c=1}^{N_c}\sum_{l=1}^{N_l} I_{l,c}}{N_c}; \quad P_{f,l} = \sum_{c=1}^{N_c} \frac{I_{l,c}}{N_c};$$

where N_c is the total number of contingencies listed, N_l is the total number of lines in the system and $I_{l,c}$ is the indicator function for line l and contingency c. The indicator function will result 0 if the line survived the cascading propagation initiate by contingency c or 1 if the line failed, e.g. due to flows redistribution leading to an overload.

4 A CASE STUDY

The IEEE RTS96 power grid is used to test the methods and the cascading model and Figure 3 displays the grid layout. The power grid data can be found in (Grigg et al. 1999) and are not reported here for sake of synthesis. In this analysis, two representative uncertainty cases, named Case A and B, are considered. In Case A, the uncertainty associated with the load demand is explicitly modelled. In the second case, CASE B, also random generation costs are accounted for, thus introducing uncertainty in the power dispatch and increasing the dimensionality of the random input space. The DC cascading model presented in section 3, is employed for the solution of the cascading problem. A predefined contingency list is selected and includes 2444 line contingencies. The list counts the full set of N-1 and N-2 line failures and a set of 1000 random N-3 line failures. To simplify comparison between uncertainty cases and the different sensitivity analysis methods, the contingency list has been kept the same throughout all the analysis (i.e. the random set of N-3 contingencies has been sampled just once).

4.1 *CASE A: Random loads*

The first uncertainty case A assumes that uncertainty affects the 17 loads in the system due to inherent variability. The analysts lack better information regarding the variability affecting the load at each node, thus, the uncertainty in *Li* is simply modelled by assuming uniform distributions. The

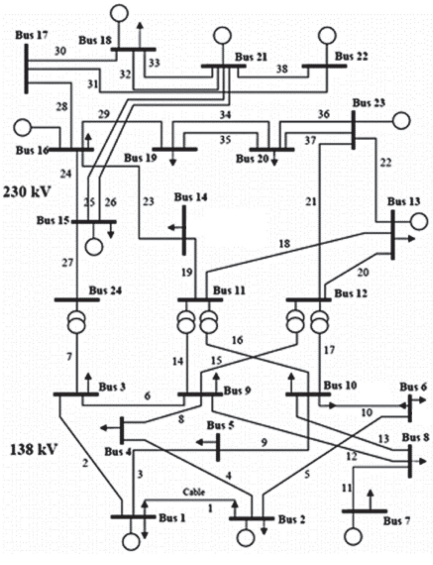

Figure 3. The IEEE RTS96 system, the connections between the 24 nodes, the lumped generators (32 generators) and the location of the aggregated loads (17 arrows).

distribution parameters have been selected to cover a range of values around the design loads and based on experts opinion:

$$L_i \sim U\left(0.5L_{d,i}, 1.2L_{d,i}\right) \quad i = 1,..,N_l$$

where $L_{d,i}$ is the design load of node i as presented in (Grigg, Wong, Albrecht, Allan, Bhavaraju, Billinton, Chen, Fong, Haddad, Kuruganty, Li, Mukerji, Pat ton, Rau, Reppen, Schneider, Shahidehpour, & Singh (1999) and the number of lines is $N_l = 17$.

Once the uncertainty sources are characterized, a preliminary uncertainty analysis is performed. Monte Carlo method is used to propagate 5e4 samples of the load profile. For each load sample, the cascading failure model is solved 2444 times, one for each contingency listed. The percentile of the demand not served, the average number of failed lines and the line outage frequencies are computed for each load sample as described in Section 3.1. The p_{95} (*DNS*) results are summarised in Figure 4. This figure presents a so-called cobweb plot, also known as parallel coordinates plot. It is a simple and effective way of visualising random input and output spaces in high dimensions. The X-axis reports the inputs loads and the percentile of the DNS (on the far right). The Y-axis reports the normalized inputs and output realisations of the Monte Carlo method. Each one of the dark dashed line in the background corresponds to one load profile realisation and corresponding The p_{95} (*DNS*) obtained through N_c model evaluations. Red solid lines are conditional samples, which highlight only the load combinations leading to the highest p_{95} (*DNS*). It can be observed, later confirmed by Morris' and Sobols' analysis, that there is a strong influence of some of the loads (e.g. in nodes 15 and 18) on the extremes of the DNS. In particular, when the power demanded in nodes 15 and 18 is small, the risk of facing severe DNS scenarios increases.

Morris and Sobol's indices have been computed aiming at better investigating which among the uncertain factors are key drivers for the output uncertainty. The Morris indices are obtained by selecting 250 random input vector realisations

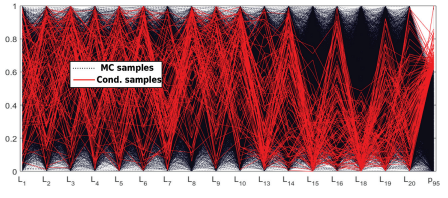

Figure 4. The parallel plot of the Monte Carlo loads and p_{95}(DNS) realizations. In red solid line the conditional samples which lead to the highest p_{95} and in the background (black dashed lines) all the MC realisations.

(saved from the MC) and computing incremental ratios δ as described in section 2.2. The Sobol's first order coefficents are obtained using given data sensitivity approaches, see ref. (Plischke, Borgonovo, & Smith 2013) for further details. This is a very convenient approach as for calculations, as the data from the MC run can be used for this and with essentially no-extra computational cost. On the other hand, total Sobol's indices require higher computational cost and in this work the Liu and Owen method (R. Liu 2006) is used for their computation.

The result relative to the DNS percentile and the average total number of line failed are presented and compared in Table 1. The Morris statistics and Sobol's main and total effect indices are also graphically presented in the $\mu - \sigma$ plot in Figure 4 and in Figure 5, respectively. Both methods identify L_{18} and L_{15} as the most influencing factors for the DNS and average number of line failures. Less relevant but, not to be neglected, is the effect of loads in nodes 8, 19 and 16. Morris analysis has the advantage of revealing an inverse relation between L_{18}, L_{15}, L_{19} and the outputs (see figure 4) which could not be revealed only using Sobol's indices. On the other hand, an increment in load 8 lead to higher risk of extreme DNS.

This result can be explained looking at the generators production profile, which is obtained solving the pre-contingency DC-SCOPF with objective

Table 1. Sobol's main and total effect mean and standard deviation for the elementary effects for the uncertainty case A for the DNS percentile and average total failed lines outputs.

	p_{95} (DNS)				$\mu(N_f)$			
	Sobol		Morris		Sobol		Morris	
	S_i	S_{Ti}	$\mu(\delta_i)$	$\sigma(\delta_i)$	S_i	S_{Ti}	$\mu(\delta_i)$	$\sigma(\delta_i)$
L_1	0.01	0.00	0.01	0.03	0.01	0.00	–0.1	0.4
L_2	0.01	0.00	0.01	0.03	0.00	0.00	–0.1	0.4
L_3	0.02	0.02	0.02	0.08	0.02	0.01	–0.5	0.7
L_4	0.01	0.00	0.01	0.03	0.01	0.00	–0.1	0.3
L_5	0.01	0.00	0.02	0.03	0.01	0.00	0.0	0.3
L_6	0.01	0.02	0.03	0.05	0.01	0.00	0.0	0.4
L_7	0.01	0.03	–0.01	0.06	0.01	0.01	0.0	0.7
L_8	0.04	0.03	0.06	0.08	0.03	0.05	0.4	0.7
L_9	0.01	0.02	0.02	0.05	0.01	0.01	–0.2	0.7
L_{10}	0.02	0.03	0.04	0.06	0.01	0.01	0.0	0.5
L_{13}	0.01	0.04	–0.01	0.09	0.01	0.03	–0.4	0.9
L_{14}	0.02	0.02	0.02	0.09	0.01	0.01	0.0	0.7
L_{15}	0.29	0.40	–0.18	0.20	0.33	0.33	–2.1	1.7
L_{16}	0.04	0.06	–0.05	0.09	0.03	0.02	–0.5	0.6
L_{18}	0.39	0.44	–0.20	0.20	0.47	0.54	–2.7	1.9
L_{19}	0.06	0.12	–0.08	0.13	0.03	0.05	–0.6	0.8
L_{20}	0.03	0.06	–0.04	0.08	0.02	0.02	–0.5	0.7

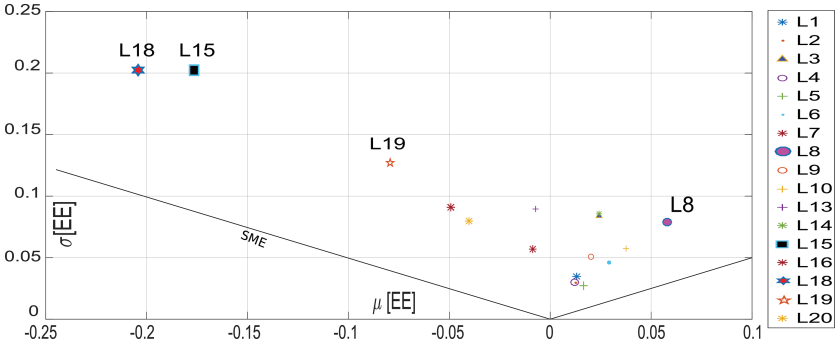

Figure 5. The Morris diagram for uncertainty case A and for the DNS percentile output. The mean and standard deviation of the EEs are reported on the X and Y axis, respectively.

of minimizing generation costs. The generators in nodes 18, 22 are associated with lower generation costs. This lead to the maximum exploitation of their production capacity, independently from the load profile realisation. Consequently, when electrical power is consumed in loco (e.g. the loads close to these generators as in 15 and 18), less power will be flowing from the 'northern' area to the 'southern' area of the network. On the other hand, if less power is demanded in, for instance, nodes 18 and 15 (or more power in 8), this increases the risk of higher loads on line such as 24, 25 and 26 which connecting the upper part of the grid with the lower part, and with it the risk of facing more severe post-contingency scenarios.

4.2 *CASE B: Random loads and generator costs*

The second uncertainty case B extends case A by accounting for generators costs uncertainties. The generation cost variability is characterised by uniform probability distributions as follows:

$$C_{g,i} \sim U(0.9,1.1) \quad i = 1,..,N_g$$

where $C_{g,i}$ is the cost of the generating unit i and the number of generators N_g is equal to 32. By assuming costs $C_{g,i}$ distributed uniformly between 0.9 and 1.1, the economic viability of the generators drastically changes if compared to case A. This lead to a higher variability in the economic dispatch, i.e. generators in nodes from 18 to 22 will sometime produce less than their maximum capacity. This case study shows the applicability of the method to larger input spaces and larger power grids. Furthermore it shows the impact of different generation profiles, in combination with load demands, on the cascading failures.

Similarly to the uncertainty case A, a Monte Carlo uncertainty propagation is performed and the Sobol's S_i indices and Morris $\mu(\delta)$ and $\sigma(\delta)$ have been calculated. The 5 most influencing factors (among the 17 loads and 32 generator costs) affecting the 95*th* percentile of the DNS are reported in Table 2. Multiple generators can be found in the same bus and to simplify the notation, the relevant costs are presented using the symbol $G_k(j)$, where j is the machine reference number within the bus k where the generator is installed. Differently from case A, load in node 8 emerged as the most relevant factor for the DNS percentile.

Table 2. Comparison between the top 5 most influencing factors according to the Sobol's main index and Morris mean and standard deviation. The output considered is the DNS percentile.

rank	S_i	$\lvert\mu(\delta)\rvert$	$\sigma(\delta)$
1	L_8	L_8	$G_{18}(1)$
2	L_3	$G_{18}(1)$	$G_{13}(2)$
3	$G_{18}(1)$	L_3	L_8
4	$G_{21}(1)$	L_6	$G_7(1)$
5	L_{18}	L_{18}	L_7

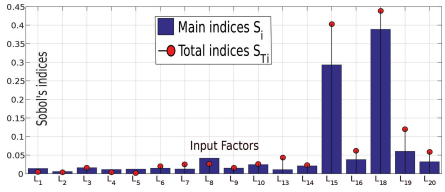

Figure 6. The Sobol s main and total effects obtained for the uncertainty case A and for the DNS percentile output.

Uncertainty in the loads and generator costs has been propagated to the line outage frequency indicator $P_{f,l}$. The resulting MC realisations are displayed using a box plot in Figure 6. The X-axes shows the lines identification number and the Y-axes presents the $P_{f,l}$ values (red markers). Each box indicates the median (the central mark) and the bottom and top edges of the box indicate the

25th and 75th percentiles, respectively. It can be observed that the line connecting node 7 to node 8 results in the higher failure frequency and that lines in the lower voltage area of the grid (ID from 1 to 13) are more prone to failure. This result is probably due to the lower thermal limit (175 MW) and to the specific combination of grid topology, design load demanded in node 7 and 8 (125 and 171 MW, respectively) and generators in node 7 maximum lumped capacity (300 MW). Thanks to the sensitivity analysis, it has been possible to clarify which are the factors responsible for this peculiar behaviour, i.e. better understanding which are the variables which are contributing the most to $P_{f,7\text{–}8}$.

Main effect sensitivity indices have been computed for each line $P_{f,l}$ to reveal which of the input factors is affecting the most their variability. Results are presented graphically with a bar plot in Figure 8 and reported in Table 3. Table 3 presents only the factors leading to relatively high S_i, i.e.

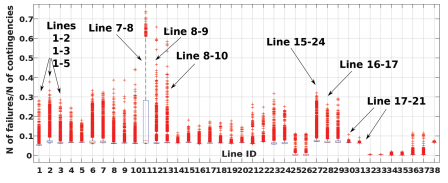

Figure 7. The box plot of the $\mathbf{P}_{f,l}$ realisations corresponding to different load and generation cost samples.

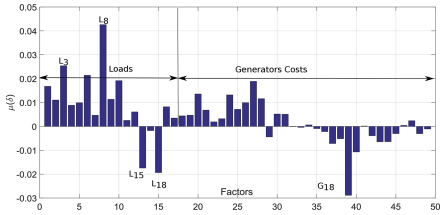

Figure 8. The tornado diagram presenting the mean o the elementary effects for the uncertain factors considered in case B.

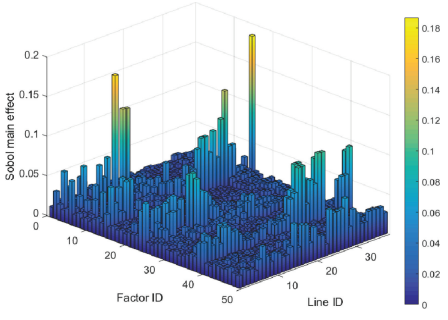

Figure 9. The $\boldsymbol{S}_i$ indices calculated for the 49 input factors and for the $\boldsymbol{P}_{fl}$ outputs. The factors from 1 to 17 are loads at different locations and last 32 are the generator costs.

Table 3. The most influencing factors for the line failure probability. Factors leading to a $\boldsymbol{S}_i > 0.08$.

From	To node	Factors
7	8	L_7, $G_7(1)$, $G_7(2)$
8	9	L_8
8	10	L_8
15	21	L_{18}, $G_{18}(1)$, $G_{21}(1)$
15	21	L_{18}, $G_{18}(1)$, $G_{21}(1)$,
16	17	L_{18}
17	18	L_{18}, G_{18},(1), G_{21} (1)
17	22	L_{18}, G_{18},(1), G_{21} (1)
21	22	L_{18}, G_{18},(1), G_{21} (1)

greater than 0.08, and the corresponding components. It can be observed that the variability in the line 7–8 outage frequency is mainly affected by uncertainty in node 7 (generators and load). On the other hand, uncertainty in L_8 is not affecting much the variance of $P_{f,7\text{–}8}$ but it is the most relevant factor for $P_{f,8\text{–}9}$, $P_{f,8\text{–}10}$.

5 DISCUSSION AND CONCLUSIONS

In this paper, the sensitivity of a cascading failures model for power grids has been analysed. Variance-based global sensitivity analysis indices, i.e. Sobol's indices, have been computed to reveal which among the uncertainty sources is affecting the most the variances of the cascading failure model output. The Morris screening indices are also obtained and compared to variance based indices to improve confidence in the results and better understand dependencies between output and factors.

Different system-level and component-level indicators have been evaluated using the cascading model. The selected metrics were the 95*th* percentile of the DNS, the average total number of line failed and the frequency of line failure for each line. The IEEE RTS96 power grid has been selected as a representative case study and used to test the applicability of the methods to a real-world system. Two uncertainty cases (Case A and Case B) have been investigated, which were characterised by an increasing dimensionality of the aleatory space.

In the Case A, only load variability has been accounted for and the result suggested that two uncertainties in the loads in node 15 and 18 are the major contributors to the extremes of the demand not served. A similar result is obtained for the average total number of line failed. Morris had the advantage of showing a negative relationship between the DNS and loads in nodes 15 and 18. In reality prices are indeed affected by uncertainty, so a sensitivity analysis that assumes fixed prices (and therefore fixed generator dispatch) might be misleading in identifying critical components in the

power grid. Thus, in the uncertainty Case B, the variability of the generator costs and loads variability are both considered. The new economic setting changed the underling behaviour of the network and, consequently, of the cascading evaluation process. The Sobol's and Morris' analysis are fairly consistent in pointing out which among the load and generators costs are the most relevant for the system output. The results are quite different compared to case A, due to the difference in the economic setting of the generators. In addition, the sensitivity of the lines outage frequency has been computed.

This analysis was performed to investigate more in detail some cascading-relevant relationships between input loads, generators costs and line failures. The results are very interesting from an engineering perspective and at least 2 results can be highlighted which are helpful in a practical context:

- The vulnerable lines (i.e. prone to failure) and the most relevant factors affecting $P_{f,l}$ are identified (using sensitivity indices). This information can be helpful to support reliability-related decision, for instance, in deciding on weather it is better to replace the line with one having higher capacity (i.e. if $P_{f,l}$ high and is similarly affected by all the input factor), or if it may be more useful to intervene on the factors affecting $P_{f,l}$ (i.e. if $P_{f,l}$ high and sensitive to just few factors);
- When the uncertainty in the loads is identified as highly relevant for a system-level indicator, it is advisable to consider actions such as allocation of distributed generators or adopt peak-shaving (load variance reduction) control methods. This can be beneficial to reduce the uncertainty in the reliability performance of the network (reducing its variance).

The framework proved to be flexible and computationally quite cheap which is a requirement for its application to more realistic large size power networks. This will be the focus of future analysis.

ACKNOWLEDGEMENTS

The authors would like to acknowledge the gracious support of this work through the EPSRC and ESRC Centre for Doctoral Training on Quantification and Management of Risk & Uncertainty in Complex Systems & Environments Grant number (EP/L015927/1).

REFERENCES

Bialek, J., E. Ciapessoni, D. Cirio, E. Cotilla-Sanchez, C. Dent, I. Dobson, P. Henneaux, P. Hines, J. Jardim, S. Miller, M. Panteli, M. Papic, A. Pitto, J. Quiros-Tortos, & D. Wu (2016, Nov). Benchmarking and validation of cascading failure analysis tools. *IEEE Transactions on Power Systems 31*(6), 4887–4900.

Bing Li, B.G. & G. Sansavini (2017, July). A genetic algorithm based calibration approach on validating cascading failure analysis. In *IEEE PES general meeting*.

Borgonovo, E. & E. Plischke (2016). Sensitivity analysis: A review of recent advances. *European Journal of Operational Research 248*(3), 869–887.

Dobson, I., B.A. Carreras, V.E. Lynch, & D.E. Newman (2001, Jan). An initial model fo complex dynamics in electric power system blackouts. In *Proceedings of the 34th Annual Hawaii International Conference on System Sciences*, pp. 710–718.

Grigg, C., P. Wong, P. Albrecht, R. Allan, M. Bhavaraju, R. Billinton, Q. Chen, C. Fong, S. Haddad, S. Kuruganty, W. Li, R. Mukerji, D. Patton, N. Rau, D. Reppen, A. Schneider, M. Shahidehpour, & C. Singh (1999, Aug). The ieee reliability test system-1996. a report prepared by the reliability test system task force of the application of probability methods subcommittee. *IEEE Transactions on Power Systems 14*(3), 1010–1020.

Kaplunovich, P. & K. Turitsyn (2016, Nov). Fast and reliable screening of n-2 contingencies. *IEEE Transactions on Power Systems 31*(6), 4243–4252.

Li, B., G. Sansavini, S. Bolognani, & F. Drfler (2016, July). Linear implicit ac pf cascading failure analysis with power system operations and automation. In *2016 IEEE Power and Energy Society General Meeting (PESGM)*, pp. 1–5.

M. Sobol, I. (1990, 01). Sensitivity estimates for nonlinear mathematical models. 2.

Morris, M.D. (1991). Factorial sampling plans for preliminary computational experiments. *Technometrics 33*(2), 161–174.

Nedic, D.P., I. Dobson, D.S. Kirschen, B.A. Carreras, & V.E. Lynch (2006). Criticality in a cascading failure blackout model. *International Journal of Electrical Power & Energy Systems 28*(9), 627–633. Selection of Papers from 15th Power Systems Computation Conference, 2005.

Patelli, E., H.J. Pradlwarter, & G.I. Schuller (2010). Global sensitivity of structural variability by random sampling. *Computer Physics Communications 181*(12), 2072–2081.

Patelli, E., M. Broggi, M. Angelis, & M. Beer (2014, June). Opencossan: An efficient open tool for dealing with epistemic and aleatory uncertainties. In *Vulnerability, Uncertainty, and Risk*, pp. 2564–2573–. American Society of Civil Engineers.

Plischke, E., E. Borgonovo, & C.L. Smith (2013). Global sensitivity measures from given data. *European Journal of Operational Research 226*(3), 536–550.

R. Liu, A.B.O. (2006). Estimating mean dimensionality of analysis of variance decompositions. *JASA 101*(474), 712721.

Rocchetta, R., E. Zio, & E. Patelli (2018). A power-flow emulator approach for resilience assessment of repairable power grids subject to weather-induced failures and data deficiency. *Applied Energy 210*(Supplement C), 339–350.

Rocchetta, R., M. Broggi, & E. Patelli (2018). Do we have enough data? robust reliability via uncertainty quantification. *Applied Mathematical Modelling 54*(Supplement C), 710–721.

Turati, P., N. Pedroni, & E. Zio (2017). Dimensionality reduction of the resilience model of a critical infrastructure network by means of elementary effects sensitivity analysis. pp. 457.